ISSN 1330-3651 (Print), ISSN 1848-6339 (Online)
https://doi.org/10.17559/TV-20181108110207
Original scientific paper

Comparison of Average Current Controlled PFC SEPIC and CUK Converter Feeding Current Controlled SRM

Erdal ŞEHİRLİ*, Yücel ÇETİNCEVİZ

Abstract: In this paper, current control of 6/4 switched reluctance motor (*SRM*) fed by both power factor correction (PFC) SEPIC and CUK converter is realised and asymmetric bridge converter is used to drive *SRM*. Furthermore, SEPIC and CUK DC-DC converters are connected in series to diode bridge rectifier in order to build PFC converters. Average current control of PFC converters is carried out by PI algorithm and both converters are operated at continuous conduction mode (CCM). Besides, switching frequency of PFC and asymmetric bridge converters is 62, 9 kHz with 5750 W power. Studies are conducted by using MATLAB/Simulink software. Total harmonic distortions (*THD*)s of grid current, grid power factor (PF) and output voltages of the converters are compared. Also, *THD*s of grid current of each converter are compared by IEEE 519-2014 standard. In addition, current waveform and flux of *SRM* phases are shown. It is validated by simulations that PFC CUK converter gives better result with 9.08% *THD*, 0.998 PF than PFC SEPIC converter having 9.61% *THD* and 0.997 PF. Furthermore, both converters provide the limit defined by standards.

Keywords: CUK; PFC; SEPIC; SRM; THD

1 INTRODUCTION

Last few decades, one of the most attractive solutions to produce mechanical energy from electrical energy is switched reluctance motor (*SRM*). Advantages of *SRM* are concentric stator winding, simple rotor without any windings, constant torque characteristic and including less power switches in its driver. However, torque ripple that can be reduced by changing converter structure may be one of its disadvantages.

On the other hand, *SRM* needs DC power for its operation and this DC power can be supplied by using single or three phase grids by rectifiers. Using diode bridge rectifiers reduces energy efficiency by causing current harmonic on grid and decreasing power factor.

To provide energy efficiency with respect to grid side, grid current should be sinusoidal and in phase with grid voltage. This operation can be realized by using PFC converters. In single phase systems, PFC converter consists of using any DC-DC converters connected series with diode bridge rectifier. As a DC-DC converter, buck, boost and buck-boost derived topologies can be used by regarding the need of output voltage.

In literature, [1] introduces fundamental knowledge about construction, operation and control of *SRM* in detail. Current control of *SRM* with hysteresis and pulse width modulation (PWM) methods is also given in [2-6]. Sliding mode and robust based current controller is realized in [7-8]. Carries out simulation of hysteresis based current control of *SRM* in MATLAB [9]. Gives summary of converter types for *SRM* [10-11]. PFC CUK converter operated in discontinuous conduction mode (DCM) with just voltage control used to feed *SRM* drive as presented in [12]. Realizes PFC modified SEPIC operated in DCM with voltage control feeding *SRM* drive [13]. *SRM* is fed by PFC boost converter in [14, 15] uses single phase half-controlled pulse width modulation (PWM) rectifier for feeding *SRM*. Presents combined PFC CUK-SEPIC based *SRM* drive operated in DCM [16]. Another study using modified quasi z-source converter that provides PFC for *SRM* drive is realized in [17]. In [18], three level T-type rectifier fed by three phase grid is used to improve PF and *THD* with Midpoint *SRM* drive.

In this paper, current control of *SRM* fed by both PFC SEPIC and CUK converter is realized. Also, *SRM* is driven by asymmetric bridge converter. Furthermore, average current controls of SEPIC and CUK PFC converter by PI controller are realized. Also, PFC CUK and SEPIC converters are operated in (CCM) whereas in [12-13, 16], such converters operated in DCM. In addition, DCM is suitable just for low power application and it provides easiness in control of PFC converter but higher current stress on the devices in converter. On the other hand, for high power application CCM is more suitable and efficient way for such converters as described in [19-20].

Applications of study in this paper are carried out by using MATLAB/Simulink. Thanks to the simulations, *THD* of grid currents, PF and output voltage are compared for each converter. Furthermore, compatibility of grid current *THD*s to IEEE 519-2014 standard is determined, current and flux of *SRM* phases are shown.

2 CURRENT CONTROL OF SWITCHED RELUCTANCE MACHINE

In this paper, current control of *SRM* is realized and the current control algorithm is shown in Fig. 1 as in [1].

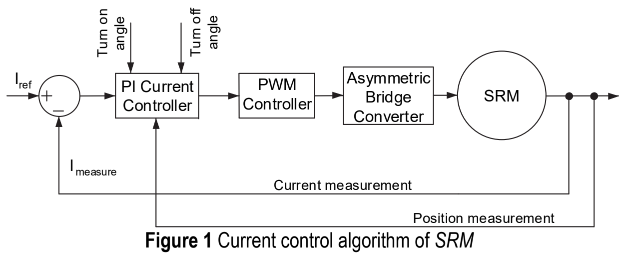

Figure 1 Current control algorithm of *SRM*

Reference current (I_{ref}) is compared with measured current ($I_{measure}$), then by using PI controller and with respect to rotor position related with turn on and turn off angles, control signal is produced and sent to PWM controller. This PWM controller produces convenient signals for converter to drive *SRM*. Governing equations including voltage and torque for *SRM* are given in Eq. (1) and Eq. (2).

$$V = R_S i + L(\theta, i)\frac{di}{dt} + \frac{dL(\theta, i)}{d\theta}\omega_m i \quad (1)$$

$$T_e = \frac{1}{2} i^2 \frac{dL(\theta, i)}{d\theta} \quad (2)$$

In Eq. (1) and Eq. (2), $L(\Theta, i)$ is self-inductance as a function of rotor position and current, T_e is electromagnetic torque, R_s is winding resistance per phase, V is applied voltage to the windings, ω_m is rotor speed in radian/s, Θ is rotor position, i is the stator current.

As a converter, asymmetric bridge converter shown in Fig. 2 is used to drive *SRM*.

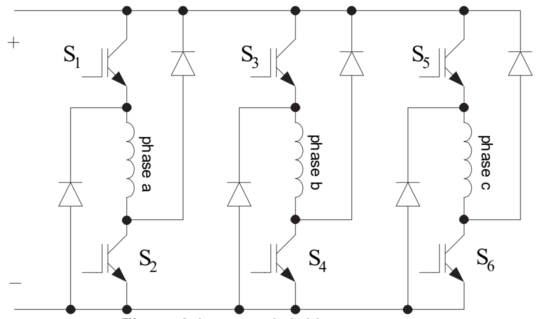

Figure 2 Asymmetric bridge converter

In asymmetric bridge converter, each phase of *SRM* consists of two power switch and diodes. Basically, the operation of converter is as follows: when the power switches are turned on, phase winding is energized and DC current flows over windings. Then, switches are turned off, winding current flows over diodes and because of applying negative voltage to winding, the energy turns back to DC power supply.

3 AVERAGE CURRENT CONTROL OF PFC CONVERTERS

In average current control of PFC, the control is realized with respect to average grid current. This control is developed for PFC boost converter as in [20]. In this paper average current control is applied to PFC SEPIC and CUK converters. To realize average current control, PFC converters are operated in CCM.

The procedure of the average current control is as follows: firstly, input side inductor current, rectified sinusoidal voltage and output dc voltage are measured. Secondly, reference current is obtained by multiplication with sinusoidal unity reference voltage acquired from rectified sinusoidal voltage and PI controller used for output voltage. Then, reference current is compared with input side inductor current and compensated by second PI controller. Lastly, regulated output of PI controller is sent to the PWM block to produce PWM signal for power switch.

3.1 Average Current Control of PFC SEPIC Converter

Average current control algorithm of PFC SEPIC converter is shown in Fig. 3. SEPIC converter is connected in series to diode bridge. Also, SEPIC converter includes two inductors that can be coupled, two capacitors and a power switch. The output voltage can be higher or lower than the input voltage depending on the duty cycle of power switch.

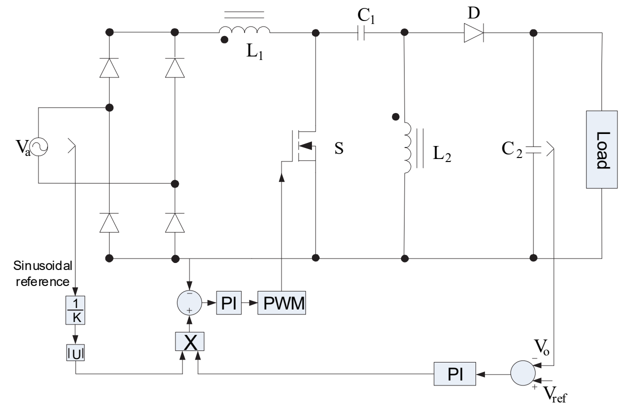

Figure 3 Average control of PFC SEPIC converter

Operation principle of SEPIC converter can be explained with respect to switch position. During the switch on interval, L_1 begins to store energy and its current increases linearly, also C_1 transfers its energy to L_2, C_2 feeds the load. During the switch off interval, input supply, L_1 transfers its energy to C_1 and to load through diode. In this interval C_1 is charged, L_2 also transfers its energy to the load.

Operation of average current control is as follows; output voltage (V_o) and reference voltage (V_{ref}) are compared and the error is regulated by PI controller. Output of PI controller is multiplied by the grid sinusoidal reference signal. By this multiplication sinusoidal reference current is obtained. Then sinusoidal reference current is compared with measured current. By using another PI controller, the current error is compensated and applied to PWM block to produce pulse for power Mosfet.

To provide operation of PFC SEPIC converter in CCM, circuit parameters can be calculated as in Eq. (3) to Eq. (6). In Eq. (3), L_{1m} and L_{2m} show the inductor value limit regarding the operation mode of CCM and DCM. For CCM operation, L_1 and L_2 values should be higher than L_{1m} and L_{2m}. Also, $\Delta I_L = I_{in} \times 40\%$. $P_o = 5750$ W, $V_o = 200$ V, $\eta = 0.9$. In Eq. (3) to Eq. (6), L_{1m}, L_{2m}; minimum inductance values of the PFC Converters, C_1 is intermediate capacitor of PFC Converters, C_2 is output capacitor of PFC Converters, D is the duty cycle, ΔI_L is inductor ripple current, P_o is output power, V_o is output voltage, η is efficiency as in [21-24].

$$L_{1m} = L_{2m} = D\frac{V_i}{2\Delta I_L f_{sw}} = \frac{0.39 \cdot 311}{2 \cdot 11.63 \cdot 62000} = 84\ \mu H \quad (3)$$

$$C_1 \ge \frac{I_o D}{\Delta V_{C1} f_{sw}} = \frac{28.75 \cdot 0.39}{10 \cdot 62000} = 18\ \mu F \quad (4)$$

$$C_2 \ge \frac{I_o D}{V_{rip} f_{sw}} = \frac{28.75 \cdot 0.39}{1 \cdot 62000} = 180\ \mu F \quad (5)$$

$$D = \frac{V_o + V_D}{V_i + V_o + V_D} = \frac{200 \cdot 0.8}{311 + 200 + 0.8} = 0.39 \quad (6)$$

3.2 Average Current Control of PFC CUK Converter

In Fig. 4 average current control of PFC CUK converter is shown. PFC CUK converter also consists of DC-DC CUK converter connected series to diode bridge. CUK converter also includes two inductors, two capacitors, diode and power switch. On the other hand, output voltage of CUK converter is reverse polarity with input voltage. Regarding the duty cycle, output voltage can be higher or lower than the input voltage.

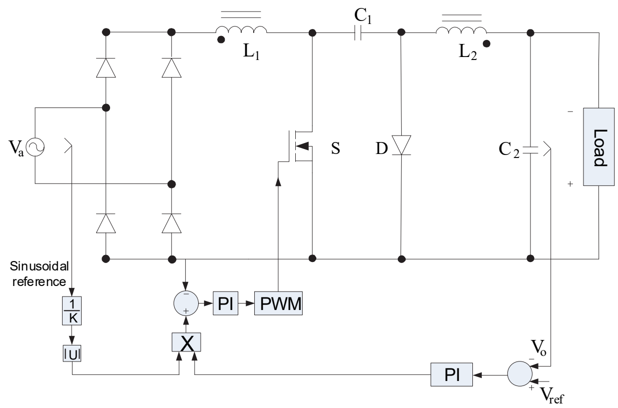

Figure 4 Average control of PFC CUK converter

Operation of CUK converter can also be summarized with respect to switch position. During the switch on interval, L_1 stores energy, its current increases linearly. Also, C_1 transfers its energy to L_2, C_2 and load. During the switch off interval, input supply and L_1 transfer their energy to the C_1, also L_2 transfers its energy to C_2 and to load.

Average current control of PFC CUK converter is realized with the same principle as PFC SEPIC converter. Also, for CCM operation of PFC CUK converter, from Eq. (3) to Eq. (6) can be used.

4 SIMULATIONS

Current control of *SRM* fed by PFC SEPIC and CUK converter is carried out by simulation study. Simulations are realized by using Matlab/Simulink. Also, simulation parameters are given in Tab. 1.

Table 1 Simulation parameters for Current Controlled *SRM* fed by both PFC SEPIC and CUK converters

PFC SEPIC			PFC CUK		
L_1, L_2	C_1	C_2	L_1, L_2	C_1	C_2
350 µH	150 µF	2200 µF	350 µH	150 µF	2200 µF

PI		PI		PI		PI	
K_p	K_i	K_p	K_i	K_p	K_i	K_p	K_i
0.1	10	0.1	0.1	0.1	10	0.1	0.1

Grid		f_{sw}		*SRM*		
V_{rms}	f_g	PFC	*SRM* Converter	Stat. P.	Cont	
				6	PI	
220 V	50 Hz	62 kHz	9 kHz	Rot. P.	K_p	K_i
				4	0.1	0.1

In this chapter, firstly current control of *SRM* is realized by using PFC SEPIC converter and then PFC CUK converter as a power supply. In order to realize comparison of the effect of each PFC converter, *THD* of grid current, grid current and grid voltage, current and flux of *SRM* are measured by means of the simulations. In addition, *THD* is calculated in Simulink by using Eq. (7).

$$THD = \sqrt{\frac{I_2^2 + I_3^2 + ... + I_n^2}{I_1^2}} \tag{7}$$

4.1 Current Control of *SRM* fed by PFC SEPIC Converter

In Fig. 5 principle diagram of PFC SEPIC converter used as a DC power supply for current controlled *SRM* is given. With average current control of PFC converter, lower *THD* and higher power factor are obtained.

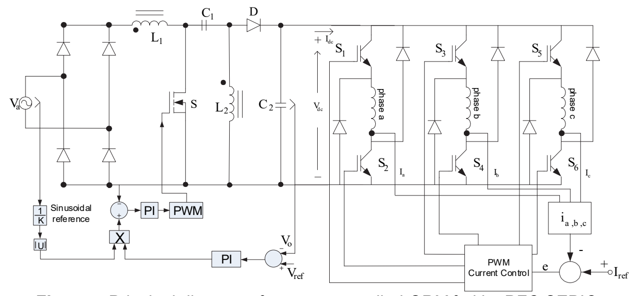

Figure 5 Principal diagram of current controlled *SRM* fed by PFC SEPIC converter

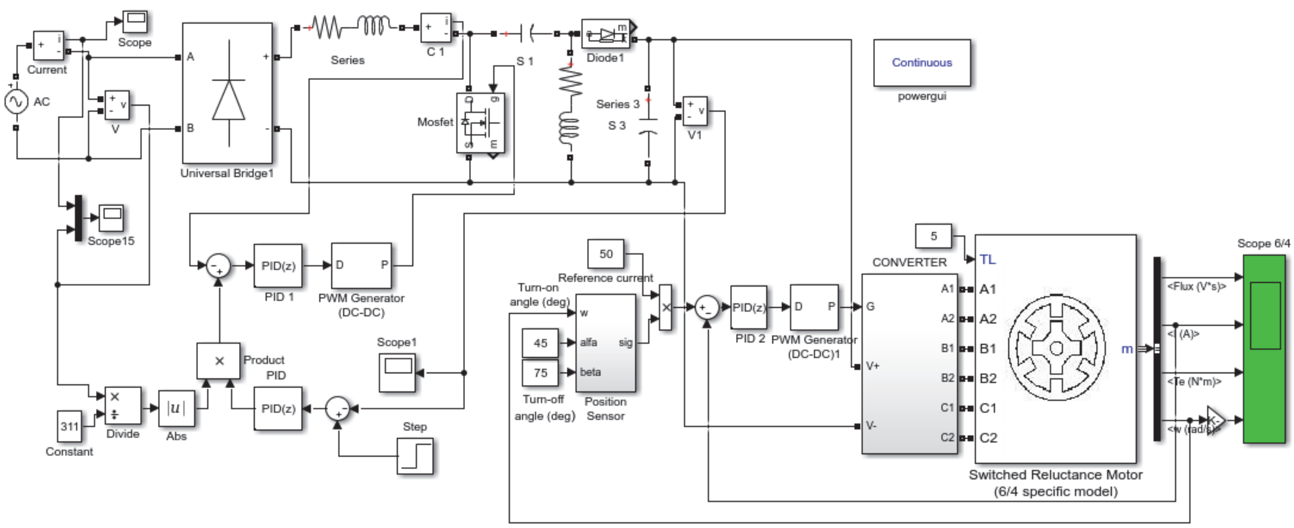

Figure 6 Simulation circuit of current controlled *SRM* fed by PFC SEPIC converter

Fig. 6 shows Matlab/Simulink simulation diagram of current controlled *SRM* fed by PFC SEPIC converter circuit. The simulation circuit in Fig. 6 is application of the principal diagram given in Fig. 5. As a power supply of reluctance machine, PFC SEPIC converter is connected. Besides, from Fig. 6, the average control algorithm given in Fig. 3 for PFC SEPIC converter is also seen.

By using PFC SEPIC converter, *THD* of grid current is obtained as 9.61% through simulation results, shown in Fig. 7. Making lower the *THD* of grid current provides better energy efficiency. So, it is concluded with the result obtained by the study that higher power quality is acquired.

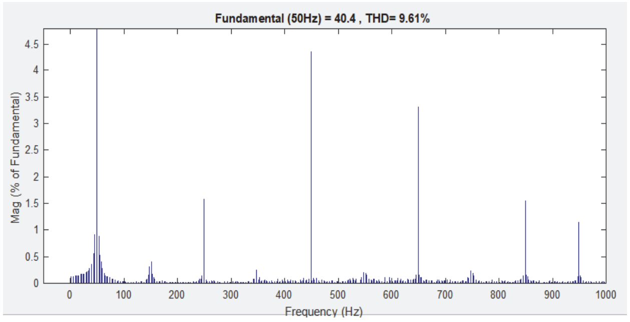

Figure 7 *THD* of grid current for PFC SEPIC converter

Grid current and grid voltage are shown in Fig. 8. It can be seen that grid voltage and current are in phase and PF is determined as 0,997. It is concluded that higher PF is obtained ensuring to draw no reactive power from grid.

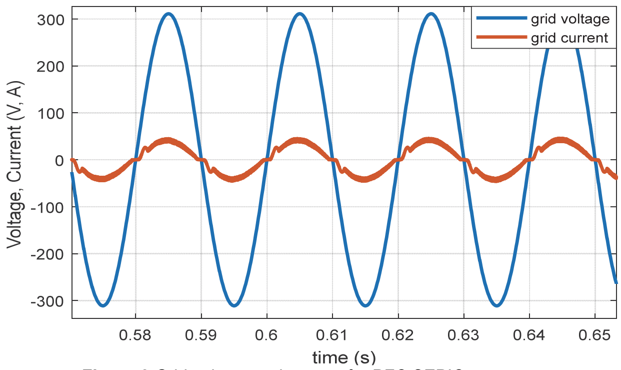

Figure 8 Grid voltage and current for PFC SEPIC converter

SRM phase currents are shown in Fig. 9 and it is observed that currents are controlled as defined in reference current that is 50 A.

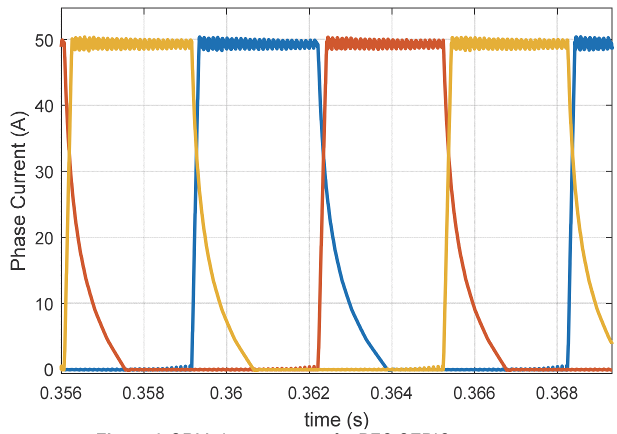

Figure 9 *SRM* phase currents for PFC SEPIC converter

Fig. 10 shows the *SRM* flux linkage per phase resulted by realizing current control of *SRM* fed by PFC SEPIC converter.

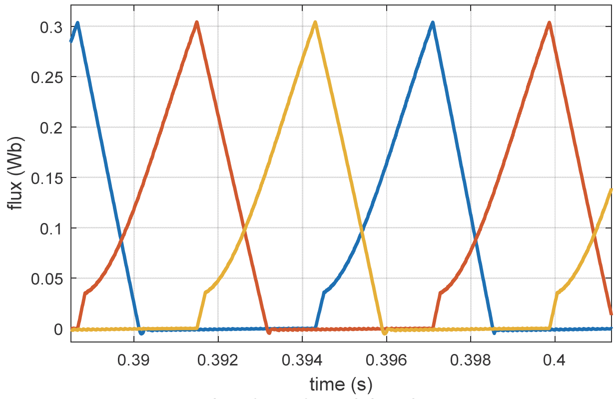

Figure 10 *SRM* fluxes for PFC SEPIC converter

4.2 Current Control of *SRM* fed by PFC CUK Converter

In Fig. 11. principle diagram of PFC CUK converter used as a DC power supply for current controlled *SRM* is given. It is seen from Fig. 11 that output DC voltage of PFC CUK converter is reverse polarity with input voltage, so output terminal of PFC CUK converter is changed to have positive polarity for *SRM* converter connection. It is also seen in Fig. 11 that PFC CUK converter has average current control algorithm given in Fig. 4. Also, asymmetric bridge converter in Fig. 2 is connected to PFC CUK converter. With average current control of PFC converter, lower *THD* and higher power factor are obtained.

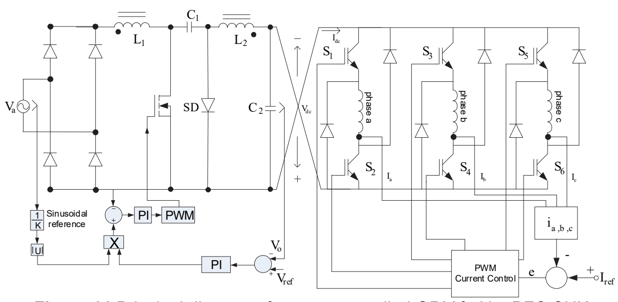

Figure 11 Principal diagram of current controlled *SRM* fed by PFC CUK converter

Fig. 12 shows Matlab/Simulink simulation diagram of current controlled *SRM* fed by PFC CUK converter circuit given in Fig. 11. It is seen by Fig. 12 that PFC CUK converter has average current control algorithm given in Fig. 4 and *SRM* has current control through PI controller.

THD of grid current is obtained as 9.08% by using PFC CUK converter through simulation and it is shown in Fig. 13. It is concluded that grid current shape is becoming sinusoidal by having lower *THD* grid current values, providing to draw energy from grid efficiently with higher PF.

Grid current and grid voltage are shown in Fig 14. It is seen that grid voltage and current are in phase and PF is determined as 0.998. It is obtained by simulations that PF is very close to unity so the PFC CUK converter does not draw reactive power from the grid while feeding *SRM* thanks to the average current control algorithm.

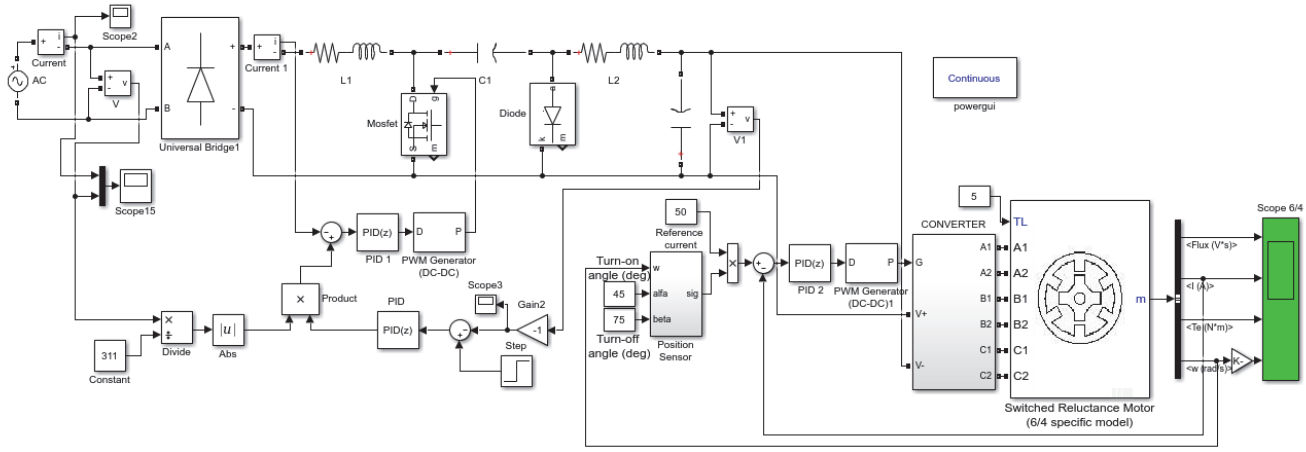

Figure 12 Simulation circuit of current controlled *SRM* fed by PFC CUK converter

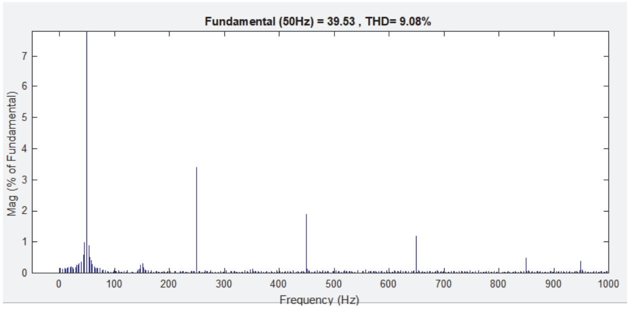

Figure 13 *THD* of grid current for PFC CUK converter

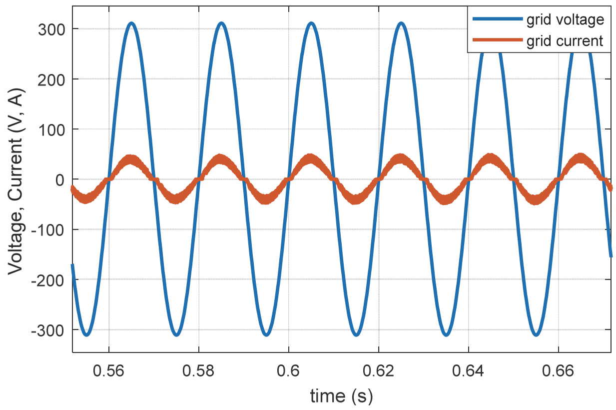

Figure 14 Grid voltage and current for PFC CUK converter

SRM phase currents are shown in Fig. 15 and it is observed that currents are controlled as desired in reference current that is 50 A.

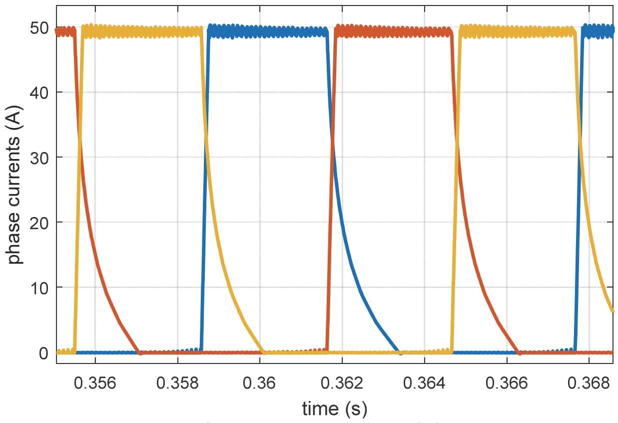

Figure 15 *SRM* phase currents for PFC CUK converter

Fig. 16 shows the *SRM* flux linkage per phase resulted by realizing current control of *SRM* fed by PFC CUK converter.

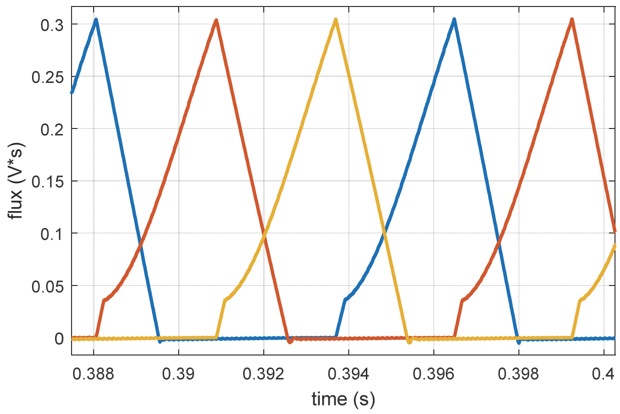

Figure 16 *SRM* fluxes for PFC CUK converter

In Fig. 17, *THD* comparison of PFC SEPIC, PFC CUK and IEEE standard 519-2014 by 50th harmonics is given and it is seen that both converters provide the standard given in [25].

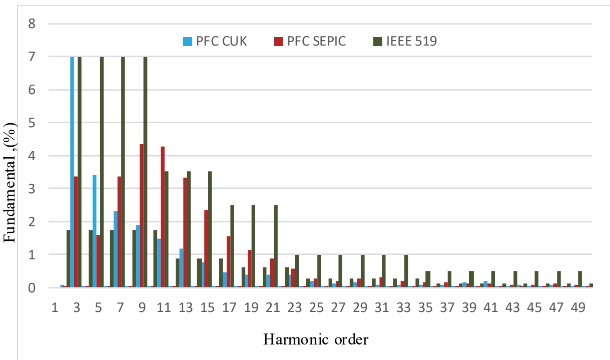

Figure 17 Comparison of current *THD*

Providing *THD* standard and having higher PF values ensure the use of energy in efficient way. Also, minimizing *THD* decreases the torque ripple and acoustic noise of *SRM*. Therefore, by means of the study in this paper, it is obtained that both PFC SEPIC and CUK converter ensure higher PF and lower *THD* in order to acquire energy efficiency.

5 CONCLUSIONS

In this paper, current control of *SRM* is realized by using asymmetric bridge converter. Besides, required DC power for asymmetric bridge converter of *SRM* is supplied by PFC SEPIC and PFC CUK converter separately. Furthermore, both PFC converters have average current control structure which is generally applied for PFC boost but not given in detail for SEPIC and CUK PFC converters in literature in order to have higher PF and lower *THD*. Thanks to the simulation studies, the effect of each PFC converter to the grid regarding *THD* and PF is investigated and results are compared.

Simulation studies are carried out by using Matlab/Simulink software. For PFC SEPIC converter, *THD* of grid current is obtained as 9.61% and PF is achieved as 0.997. However, *THD* of grid current for PFC CUK converter is obtained as 9.08% and PF is acquired as 0.998. It is observed by simulation results that PFC CUK converter gives better result than PFC SEPIC converter regarding PF and *THD*. Nonetheless, supplying DC voltage that is reverse polarity with respect to input voltage can be considered as a weak way of PFC CUK converter. However, both PFC converters provide the limit defined by the standard. It is also concluded that both PFC SEPIC and CUK converters are a good alternative to supply DC power for *SRM* converter with higher PF and lower *THD*.

It is also shown by simulation studies that by using both PFC converters, current control of *SRM* is achieved as is desired.

6 REFERENCES

[1] Krishnan, R. (2001). *Switched Reluctance Motor Drives,* New Jersey, USA: CRC Press.

[2] Husain, I. & Ehsani, M. (1996). Torque ripple minimization in switched reluctance motor drives by PWM current control. *IEEE Transactions on Power Electronics*, *11*(1), 83-88. https://doi.org/10.1109/63.484420

[3] Geldhof, K. R., Vyncke, T. J., De Belie, F. M. L. L., Vandevelde, L., Melkebeek, J. A. A., & Boel, R. K. (2007). Embedded runge-kutta methods for integration of a current control loop in an *SRM* dynamic finite element model. *IET Science, Measurement & Technology*, *1*(1), 17-20. https://doi.org/10.1049/iet-smt:20060026

[4] Lee, D. H., Lee, J. H., & Ahn, J. W. (2011). Current control of a high speed *SRM* with an advanced 4-level converter. *Proceeding of 8th International Conference on Power Electronics,* 109-114. https://doi.org/10.1109/ICPE.2011.5944558

[5] Chun, G., Jianhua, W., Shiyou, Y., & Yihua, H. (2015). Phase current reconstruction of switched reluctance motors from dc-link current under double high-frequency pulses injection. *IEEE Transactions on Industrial Electronics*, *62*(5), 3265-3276. https://doi.org/10.1109/TIE.2014.2364153

[6] Fei, P., Jin, Y., & Emadi, A. (2016). A digital PWM current controller for switched reluctance motor drives. *IEEE Transactions on Power Electronics*, *31*(10), 7087-7098. https://doi.org/10.1109/TPEL.2015.2510028

[7] Jin, Y., Malysz, P., & Emadi, A. (2015). A fixed switching frequency integral sliding mode current controller for switched reluctance motor drives. *IEEE Journal of Emerging and Selected Topics in Power Electronics*, *3*(2), 381-394. https://doi.org/10.1109/JESTPE.2014.2357717

[8] Krishnamurthy, P., Wenzhe, L., Khorrami, F., & Keyhani, A. (2009). Robust force control of an *SRM*-based electromechanical brake and experimental results. *IEEE Transactions on Control System Technology*, *17*(6), 1306-1317. https://doi.org/10.1109/TCST.2008.2006908

[9] Hoang, L. H. & Chakir, M. (2010). Optimizing the performance of a switched reluctance generator by simulation. *Proceeding of the XIX International Conference on Electrical Machines-ICEM 2010*, 1-6. https://doi.org/10.1109/ICELMACH.2010.5608165

[10] Ha, K., Lee, C., Kim, J., Krishnan, R., & Oh, S. G. (2007). Design and development of low cost and high efficiency variable speed drive system with switched reluctance motor. *IEEE Transactions on Industrial Application*, *40*(3), 703-713. https://doi.org/10.1109/TIA.2007.895744

[11] Vukosavic, S. & Stefanovic, V. R. (1991). *SRM* inverter topologies: A comparative evaluation. *IEEE Transactions on Industrial Application*, *27*(6), 1034-1047. https://doi.org/10.1109/28.108453

[12] Anand, A. & Singh, B. (2017). Design and implementation of PFC CUK converter fed *SRM* drive. *IET Power Electronics*, *10*(12), 1539-1549. https://doi.org/10.1049/iet-pel.2016.1039

[13] Singh, B. & Anand, A. (2018). Power factor correction in modified SEPIC fed switched reluctance motor drives. *IEEE Transactions on Industry Applications*, *54*(5), 4494-4505. https://doi.org/10.1109/TIA.2018.2840079

[14] Chai, Y. J. & Liaw, C. M. (2009). Development of a switched-reluctance motor drive with PFC front end. *IEEE Transactions on Energy Conversion*, *24*(1), 30-42. https://doi.org/10.1109/TEC.2008.2002328

[15] Huang, H. N., Hu, K. W., & Liaw, C. M. (2017). Switch-mode rectifier fed switched-reluctance motor drive with dynamic commutation shifting using DC-link current. *IET Electric Power Applications*, *11*(4), 640-652. https://doi.org/10.1049/iet-epa.2016.0783

[16] Anand, A. & Singh, B. (2018). Power factor correction in CUK-SEPIC-based dual-output-converter-fed *SRM* drive. *IEEE Transactions on Industrial Electronics*, *65*(2), 1117-1127. https://doi.org/10.1109/TIE.2017.2733482

[17] Mohamedi, M., Rashidi, A., Nejad S. M. S., & Ebrahimi, M. (2018). A switched reluctance motor drive based on quasi z-source converter with voltage regulation and power factor correction. *IEEE Transactions on Industrial Electronics*, *65*(10), 8330-8339. https://doi.org/10.1109/TIE.2017.2787553

[18] Tang, Y., He, Y., Wang F., Ling, G., Rodriguez, J., & Kennel, R. (2021). A Centralized control strategy for grid-connected high-speed switched reluctance motor drive system with power factor correction. *IEEE Transactions on Energy Conversion*, *36*(3), 2163-2172. https://doi.org/ 10.1109/TEC.2021.3051167

[19] Zhang, J., Jovanovic, M. M, & Lee, F. C. (1999). Comparison between CCM single-stage and two-stage boost PFC converters. *Proceedings of 14th Annual Applied Power Electronics Conference and Exposition Transactions on Industrial Electronics*, 335-341. https://doi.org/10.1109/APEC.1999.749674

[20] Rosetto, L., Spiazzi, G., & Tenti, P. (1994). Control techniques for power factor correction converters. *Proceedings of Power Electronics and Motion Control Conference Proceedings*, 1310-1318. http://www.dei.unipd.it/~pel/Articoli/1994/Pemc /Pemc94.pdf

[21] Babaei, E. & Mahmodieh, M. E. S. (2018). Calculation of Output Voltage Ripple and Design Considerations of SEPIC Converter. *IEEE Transactions on Industrial Electronics*, *61*(3), 1213-1222. https://doi.org/10.1109/TIE.2013.2262748

[22] Zhang, D. (2013). *AN-1484 Designing a SEPIC Converter*. Texas Instruments. https://www.ti.com/lit/an/snva168e/snva168e.pdf

[23] Fallin, J. (2008). *Designing DC/DC Converters Based on SEPIC Converter*. Texas Instruments. https://www.ti.com/ lit/an/ slyt309/ slyt309.pdf
[24] Texas Instruments. (2015). *LM2611 1.4 MHz CUK Converter.* Texas instruments. https://www.ti.com/lit/ds/symlink/lm2611.pdf
[25] *519-2014 - IEEE Recommended Practice and Requirements for Harmonic Control in Electric Power Systems.* (2014). IEEE. https://doi.org/10.1109/IEEESTD.2014.6826459

Contact information:

Erdal ŞEHİRLİ, PhD Lecturer
(Corresponding author)
Electrical and Electronics Engineering Department,
Kastamonu University,
Kuzeykent, Kastamonu, 37150 Turkey
E-mail: esehirli@kastamonu.edu.tr

Yücel ÇETİNCEVİZ, PhD Lecturer
Electrical and Electronics Engineering Department,
Kastamonu University,
Kuzeykent, Kastamonu, 37150 Turkey
E-mail: ycetinceviz@kastamonu.edu.tr